Chemistry & Biology, Vol. 9, 907–913, August, 2002, ©2002 Elsevier Science Ltd. All rights reserved. PII S1074-5521(02)00185-0

Controlling Protein Activity with Ligand-Regulated RNA Aptamers

Momchilo Vuyisich and Peter A. Beal[1]
Department of Chemistry
University of Utah
Salt Lake City, Utah 84112

Summary

Controlling the activity of a protein is necessary for defining its function in vivo. RNA aptamers are capable of inhibiting proteins with high affinity and specificity, but this effect is not readily reversible. We describe a general method for discovering aptamers that bind and inhibit their target protein, but addition of a specific small molecule disrupts the protein-RNA complex. A SELEX protocol was used to raise RNA aptamers to the DNA repair enzyme, formamidopyrimidine glycosylase (Fpg), and neomycin was employed in each round to dissociate Fpg-bound RNAs. We identified an RNA molecule able to completely inhibit Fpg at 100 nM concentration. Importantly, Fpg activity is recovered by the addition of neomycin. We envision these ligand-regulated aptamers (LIRAs) as valuable tools in the study of biological phenomena in which the timing of molecular events is critical.

Introduction

Based on the current data from the human genome project, the total number of genes is estimated to be between 35,000 and 45,000 [1]. While functional genetics has made great progress in deciphering the roles of many individual gene products, the process can be slow and has limitations. In recent years, the field of chemical genetics has developed new ways of studying protein function by modulating a target protein's activity with specific inhibitors [2]. A number of groups have performed selections from combinatorial libraries and identified small molecule inhibitors that target specific proteins [3–7]. Alternative strategies to the selective inhibition of protein targets have also been developed. In one approach, the active site of the protein is altered by mutation, and a rationally designed variant of a known inhibitor of the wild-type protein is used that is structurally complementary only to the mutant [8]. Systematic evolution of ligands by exponential enrichment (SELEX) has also been used to discover RNA molecules (aptamers) that act as protein inhibitors and exhibit high affinity and specificity for their targets [9–11]. Given that extremely diverse RNA libraries can be screened and mutations arising during the selection allow the RNA to evolve the desired properties, this strategy is an attractive one for the discovery of selective protein inhibitors [12]. RNA aptamer inhibitors of proteins have also been expressed inside eukaryotic cells and shown to elicit an inhibitory effect on their target proteins in the cellular environment [13–15]. In addition, ligand binding aptamers inserted into the 5′ UTR of messenger RNA allow for control of gene expression inside living cells [16].

One potential drawback of the RNA aptamer approach described above is that once the aptamer is expressed in the cell and the target protein is inhibited, activity can no longer be precisely controlled. Tight temporal regulation of protein activity may be desired in certain instances when the timing of events is critical, such as during the cell cycle or in early development [17–19]. Having an expressed but nonfunctional (inhibited) gene product, then activating it at a desired point in time would be valuable in these cases. In such a system, one could monitor cellular activities or pathways while the target protein is inhibited, then activate the protein and detect changes.

We reasoned that this goal might be accomplished with an RNA aptamer whose binding to the protein was itself regulated by an organic small molecule. Thus, a selected RNA could bind and inhibit the target protein. At a desired point in time, addition of the small molecule (inducer) would disrupt the RNA-protein complex, leading to the functional protein (Figure 1). Our approach was to employ a small molecule in an elution step during the SELEX protocol, leading to the amplification of RNAs that bind a target protein but dissociate from it in the presence of a small molecule (Figure 2). We refer to these RNAs as "ligand-regulated aptamers," or LIRAs. In systems that employ LIRAs, a functional protein can be inhibited for a specific period of time as the inhibition is temporally controlled by adding the inducer.

When considering the desired properties of a ligand-regulated inhibitor, we realized that RNA structures should be capable of performing such tasks. In addition to aptamers' ability to bind a variety of proteins, in vitro selected RNAs are capable of recognizing small organic molecules with high affinity and specificity [11, 20, 21]. Also, there are several examples of ribozymes whose activity can be regulated by the presence of small molecules called effectors [22–25]. These effector-regulated ribozymes have been discovered using SELEX, where a fixed catalytic domain and a known small molecule binding domain are connected via a randomized RNA "communication module." Alternatively, the communication module and the catalytic domain can be fixed, and the small molecule binding domain can be randomized, thus selecting for new effector molecules [26]. In our approach, all parts of the LIRA are randomized, and we simultaneously select for an aptamer that can bind both the protein target and a small molecule.

For an initial proof of principle experiment, we chose both a target protein and a potential inducer that are predisposed to bind nucleic acids. For the protein target, we employed the DNA repair enzyme formamidopyrimidine glycosylase (Fpg), also known as MutM [27, 28]. This enzyme recognizes 8-oxo-dG lesions in DNA and removes the oxidized nucleotides from the strand, using its N-glycosylase and AP-lyase activities [29, 30]. Our choice for the small molecule was neomycin, which be-

[1]Correspondence: beal@chemistry.utah.edu

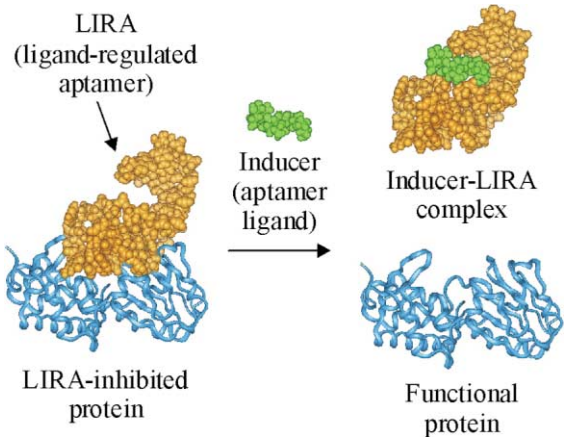

Figure 1. A Schematic Depiction of the Properties of Ligand-Regulated Aptamers

A protein of interest is bound and inhibited by a ligand-regulated aptamer (LIRA). The inhibition is relieved by the addition of a ligand (inducer) that dissociates the LIRA-protein complex.

longs to the aminoglycoside class of antibiotics. These molecules have been shown to bind many naturally occurring RNA ligands [31–33]. In addition, neomycin was used as a SELEX target and shown to bind a specific sequence motif in RNA [34].

Results

SELEX Results

Recombinant *E. coli* formamidopyrimidine glycosylase (Fpg) enzyme was selected as our initial protein target [27, 29]. This nucleic acid binding protein is readily overexpressed, easily purified, and has a simple, well established assay for activity [28, 35, 36]. A sequence-randomized RNA library was allowed to bind Fpg in solution followed by separation of free RNA from the Fpg-bound species using filter paper. In the first six rounds, a nonspecific urea buffer was used for elutions of Fpg-bound RNAs. In round seven, the RNA pool was split and used for two parallel selections. In the N selection, neomycin was used in the elution step. Therefore, only the RNAs that bound Fpg but dissociated in the presence of the aminoglycoside were collected and amplified. In the U

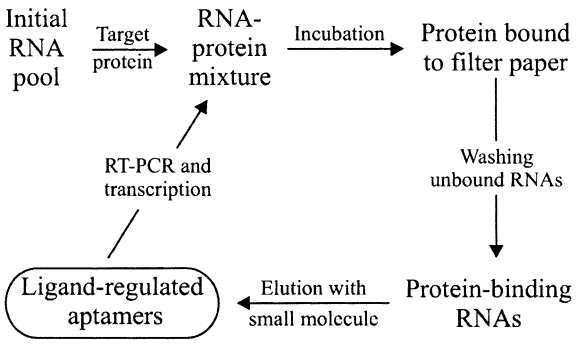

Figure 2. Selection Strategy for the Discovery of Ligand-Regulated Aptamers to Proteins

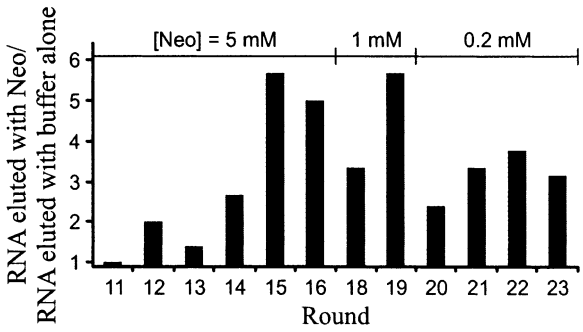

Figure 3. Progress of the N Selection from Rounds 11–23

The ratio of the RNA amount eluted with wash buffer/neomycin and RNA eluted with wash buffer alone is plotted as a function of the round number.

selection, urea continued to be used in the elution step, selecting any RNA structure with affinity for Fpg.

During the N selection, the progress by round was measured by calculating the ratio of the amount of RNA eluted with 5 mM neomycin in the wash buffer and RNA eluted with wash buffer alone. This ratio climbed to near six in round 15 (Figure 3). In round 18, the neomycin concentration was reduced to 1 mM in order to select for aptamers more sensitive to neomycin. The ratio dropped but quickly recovered (Figure 3). Finally, 200 μM neomycin was used in the last four rounds, after which the cDNA library was cloned, and the RNAs from this pool were designated N aptamers.

The U selection was performed for a total of 14 rounds, after which the library was tested for its ability to inhibit Fpg. Under single-turnover conditions, 1 μM library from the U selection after fourteen rounds completely inhibited the enzyme, whereas the same concentration of the initial RNA pool had no effect on Fpg. We cloned the cDNA pool at this stage and refer to the RNA clones from this selection as U aptamers.

We tested the ability of the RNA pool from the 23rd N selection to inhibit Fpg in the presence of neomycin. As a control, we used the RNA pool from the fourteenth round of the U selection. The pool from the N selection was indeed more sensitive to neomycin (by an order of magnitude) than the U selection pool, which was never pressured to dissociate from Fpg in the presence of the aminoglycoside. After cloning, we tested 5 N and 9 U aptamers for their ability to inhibit Fpg with and without neomycin. In general, N aptamers were more sensitive to neomycin than U selection aptamers.

Aptamer Binding to Fpg

We tested several aptamers from each selection for their ability to bind and inhibit Fpg. Based on these results, we selected two clones (one from each selection) which bound Fpg with similar affinities and possessed similar inhibitory activities. We designated these the neomycin-regulated aptamer (N1) and the control aptamer (U1). Using a quantitative filter binding assay, the K_D was determined to be 7.5 ± 1.6 nM for N1 and 2.7 ± 0.9 nM for U1. Our steady-state experiments revealed complete inhibition of Fpg activity by both N1 and U1 aptamers at 100 nM concentration.

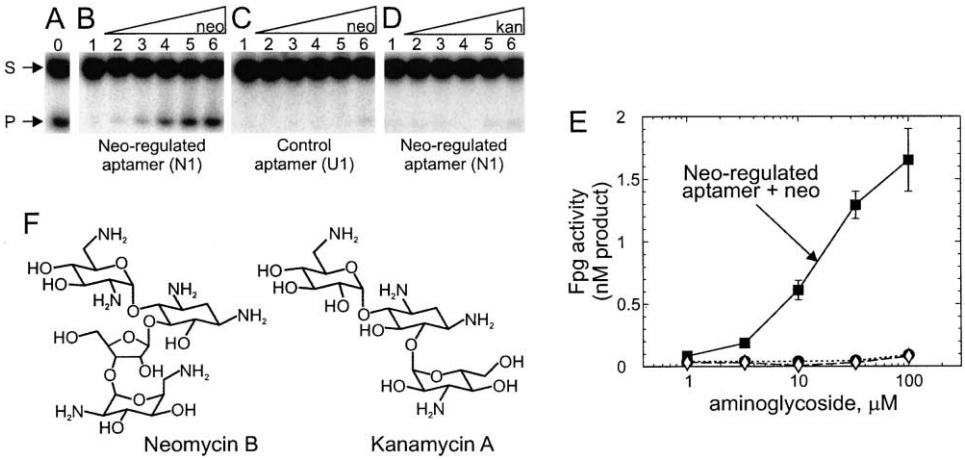

Figure 4. Inhibition of Fpg by N1 Aptamer

(A) Fpg activity under steady-state conditions, where S denotes the substrate and P denotes the product band (see Experimental Procedures).
(B) Fpg activity in the presence of 100 nM N1 aptamer. Lanes 2–6 had the following concentrations of neomycin: 1 μM, 3 μM, 10 μM, 30 μM, and 100 μM, respectively.
(C) Same reactions as in (B), with U1 aptamer at 100 nM instead of the N1 aptamer.
(D) Same reactions as in (B), with kanamycin instead of neomycin (same concentrations).
(E) Graphical depiction of data from (B)–(D). Data from (B) are represented by squares, from (C) by circles, and from (D) by diamonds.
(F) Structures of two aminoglycosides used in this study, neomycin B and kanamycin A.

Effects of Neomycin on Aptamer Inhibition of Fpg

We wished to determine the relative response of the two selected aptamers to the presence of neomycin. Reaction components (aptamer, Fpg, and an aminoglycoside antibiotic) were incubated together, followed by the addition of labeled Fpg substrate under steady-state conditions. Full inhibition of the Fpg activity is observed with the N1 aptamer present at 100 nM concentration (Figure 4B, lane 1). As increasing concentrations of neomycin are added, the aptamer inhibition of Fpg is relieved (Figure 4B, lanes 2–6). At 100 μM neomycin, the Fpg activity approaches its maximum, in which ~2 nM product is observed (compare lanes 0 and 6). The neomycin rescue was not observed when the control aptamer (U1), which binds Fpg with similar affinity as N1, was used to inhibit the enzyme (Figure 4C). To determine if the disruption of the N1-Fpg complex is specific to neomycin, we repeated the experiment with the structurally similar aminoglycoside kanamycin (Figure 4F). Importantly, this related aminoglycoside is unable to interfere with the inhibitory activity of the N1 aptamer under these conditions (Figure 4D). The amount of product (nM) in Figures 4B–4D was quantified and plotted as a function of aminoglycoside concentration (Figure 4E).

Secondary Structure of the Neomycin-Regulated Aptamer

Sequencing of cDNA for the N1 aptamer allowed us to predict the RNA's secondary structure using the computer program MFOLD (http://bioinfo.math.rpi.edu/~mfold/rna/form1.cgi) (Figure 5B) [37]. To test the predicted model, we used ribonucleases specific for single- and double-stranded RNA, which included S1, V1, and T1. Figure 5A shows cleavage of N1 aptamer by S1 and V1 ribonucleases under native conditions. Major cleavage sites on the RNA are mapped onto the predicted secondary structure of the aptamer (Figure 5B). The mapping also includes the major cleavage sites of T1 ribonuclease digest under native conditions, which are shown in Figure 6A, lane 4. In general, the reactivity observed with the different ribonucleases agrees with the predicted secondary structure.

Footprinting of Fpg and Neomycin on the Neomycin-Regulated Aptamer

In order to locate the binding sites for Fpg and neomycin on the N1 aptamer, cleavage protection assays (footprinting) were performed. We utilized several ribonucleases (S1, V1, T1, and P1) for this purpose, and the results can be best demonstrated by ribonuclease T1 footprinting (Figure 6). Figure 6A shows that cleavage by T1 diminishes at G27 as neomycin is added (lanes 5–13). Lanes 14–19 show a decrease in T1 cleavage from G27 to G35 in response to increasing amounts of Fpg. Thus, Fpg and neomycin bind the N1 aptamer at apparently overlapping sites at the junction between a stem structure and a single-stranded loop near the center of the RNA strand (Figure 6B). When protection from T1 cleavage is converted to fraction RNA bound by neomycin, the data can be fitted using a single-site binding equation, which results in a K_d of 0.94 ± 0.06 μM (Figure 6C).

The Importance of the 3′ Stem-Loop of N1 Aptamer

From the predicted secondary structure and the location of Fpg and neomycin binding sites on N1 aptamer, the 3′ stem-loop of the RNA (nucleotides 60–91) appeared to be dispensable. To test this idea, we prepared two deletion mutants of the N1 aptamer, comprising 59 or 66 nucleotides from the 5′ end. Neither of these RNAs was able to inhibit Fpg at 200 nM concentration. This

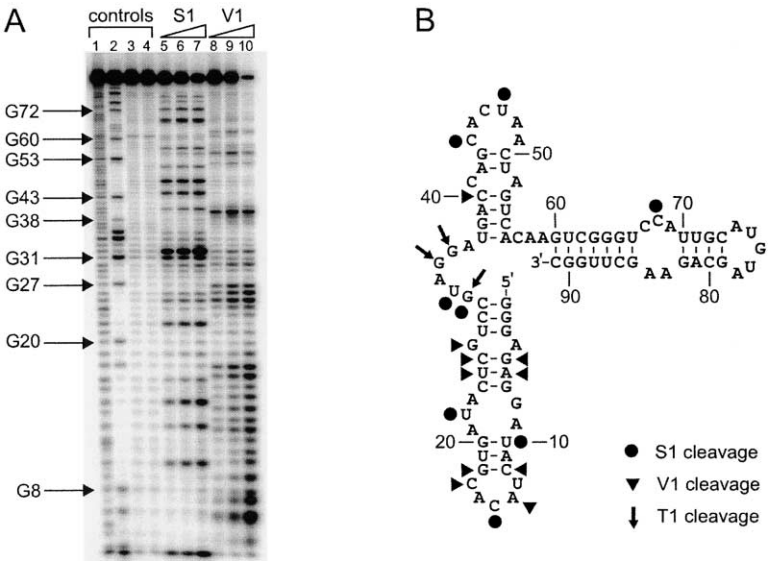

Figure 5. N1 Aptamer Secondary Structure Prediction and Structure Probing

(A) Ten percent polyacrylamide gel showing cleavage of N1 by single-strand (S1) and double-strand (V1) specific ribonucleases. Lane 1, alkaline hydrolysis; lane 2, G lane (RNase T1); lane 3, RNA only; lane 4, RNA + 0.1 mM $ZnCl_2$; lane 5, RNA + 2 u/μL S1; lane 6, RNA + 5 u/μL S1; lane 7, RNA + 10 u/μL S1; lane 8, RNA + 1 u/mL V1; lane 9, RNA + 2 u/mL V1; lane 10, RNA + 10 u/mL V1.

(B) Secondary structure of N1 aptamer predicted by MFOLD. Major cleavage sites of S1, V1, and T1 ribonucleases are represented by circles, triangles, and arrows, respectively. The major cleavage sites identified for ribonucleases S1 and V1 are those observed in lanes 6 and 9, respectively.

result indicates that the 3′ stem-loop is important for the inhibitory effect of N1, perhaps in maintaining the aptamer's three-dimensional structure.

Discussion

Several chemical genetics methods have been developed to delineate the functions of gene products that complement existing functional genetics approaches [2–8, 12]. One of these methods relies on the selection of an RNA aptamer inhibitor of the protein, which is then expressed inside the target cell [12]. These RNA molecules are able to specifically block the function of a gene product. In this work, we build on this idea and present a method for temporally controlling the activity of a gene product which involves an RNA aptamer as

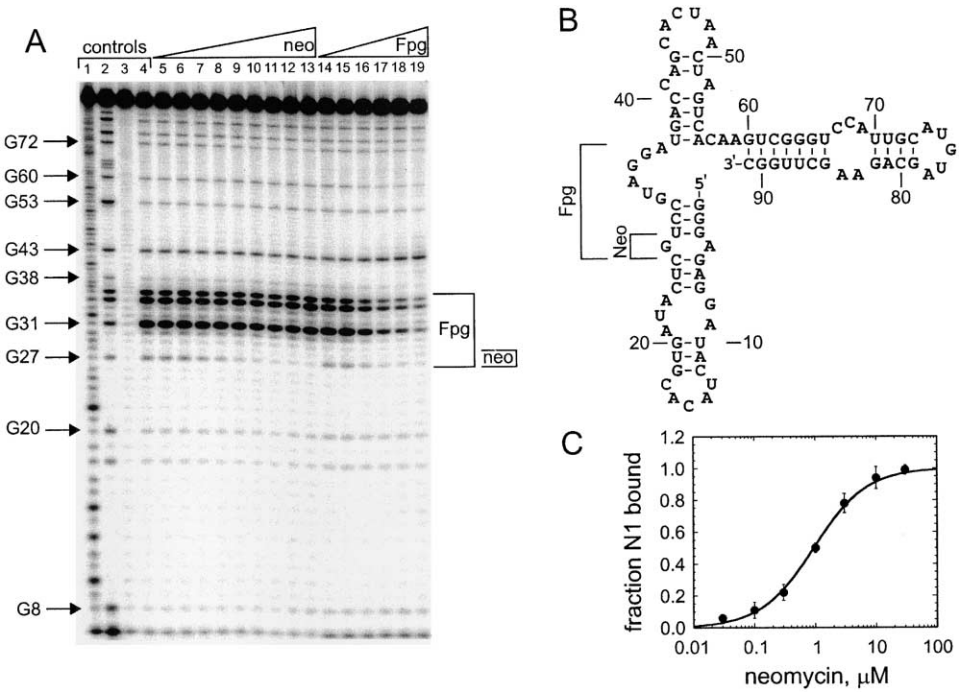

Figure 6. Fpg and Neomycin Footprints on N1 Aptamer

(A) Ten percent polyacrylamide gel showing T1 RNase cleavage of N1 in the presence of Fpg and neomycin. Lane 1, alkaline hydrolysis; lane 2, G lane (RNase T1); lane 3, RNA only; lanes 4–19, 1 u/mL T1 RNase; lanes 5–13, increasing concentrations of neomycin as follows: 0.03 μM, 0.1 μM, 0.3 μM, 1 μM, 3 μM, 10 μM, 30 μM, 100 μM, 300 μM; lanes 14–19, increasing concentrations of Fpg as follows: 0.3 nM, 1 nM, 3 nM, 10 nM, 30 nM, 100 nM.

(B) N1 secondary structure with brackets showing Fpg and neomycin binding sites.

(C) Fraction N1 bound by neomycin is plotted as a function of the aminoglycoside concentration.

the inhibitor of the target protein and a small molecule capable of relieving that inhibition (the inducer).

We utilized the SELEX method to evolve RNA aptamers that bind the DNA repair protein formamidopyrimidine glycosylase, Fpg [11]. In addition, we introduced a step in the selection where RNA was eluted from filter-bound protein using the aminoglycoside antibiotic neomycin. This was the critical step that allowed us to collect and amplify only the RNA structures that satisfied two criteria: (1) the RNA must bind Fpg, and (2) the Fpg-bound RNA must dissociate from the protein in the presence of neomycin. After 23 rounds of SELEX and initial characterization of five clones, we further investigated the properties of clone N1, a 91-mer RNA aptamer. To ensure that the features of the N1 RNA were not arrived at by chance, we also performed a selection with Fpg using a highly stringent, nonspecific elution buffer (see Experimental Procedures). One of the clones from this selection (designated U1) bound Fpg with an affinity similar to that of N1 and was used for comparison to N1.

Although both N1 and U1 aptamers bind and inhibit Fpg similarly, the two aptamers showed dramatically different inhibitory activities in the presence of neomycin (Figure 4). While most of the Fpg activity was rescued from inhibition by N1 in the presence of 100 μM neomycin, the same concentration of the aminoglycoside had only a minimal effect on Fpg inhibition by the U1 aptamer. Furthermore, no appreciable rescue of Fpg activity was observed with 100 μM kanamycin, an aminoglycoside structurally related to neomycin. Thus, the ability of neomycin to rescue Fpg activity from the inhibitory effect of the N1 aptamer is dependent both on the structure of the evolved RNA aptamer and the small molecule used during the selection.

To shed light on the mechanism by which neomycin regulates the N1 aptamer, we carried out secondary structure prediction, structure probing studies, and footprinting with this RNA. These experiments suggested a probable secondary structure as well as identified binding sites for Fpg and neomycin on the RNA. It is apparent that the selection carried out led to the isolation of an aptamer that had overlapping binding sites for Fpg and neomycin, suggesting the mode of action of neomycin is a competitive one (Figure 6). Interestingly, the sequence at the neomycin binding site is similar to those previously implicated in binding aminoglycosides. For example, the 5′-GU-3′ step, which is present in N1 aptamer as G27 and U28, has recently been shown to bind the aminoglycoside deoxystreptamine ring [32]. In addition, neomycin binding aptamers contain G-rich regions adjacent to a bulge, which is similar to the 5′ end of N1 aptamer [34].

The method developed here for discovering a LIRA/small molecule pair is potentially general for any target protein or protein domain. Such inhibitor/inducer pairs could be used to inhibit proteins in vivo, then relieve the inhibition at desired points in time. This would be valuable for the study of cellular phenomena in which the timing of molecular events is critical, such as in cell cycle regulation, circadian clocks, or controlling cell fates during early development. A system that includes neomycin as the inducer is probably not suitable for a cell biology application due to its toxicity [38]. However, we believe this proof of principle exercise will pave the way for applications involving proteins whose roles are poorly understood and small molecules that are cell permeable and nontoxic. In the example reported here, we chose to use the presence of a small molecule as the switch in protein activity. In principle, other conditions could also have been chosen. For instance, an aptamer that dissociates from the target protein in the presence or absence of a specific metal ion or by a change in pH could lead to other means by which the target protein could be regulated [39]. This could lead to a method to regulate protein activity only in certain cellular compartments or only in cells responding to a specific environmental stimulus.

In addition to these chemical genetic applications, the discovery of new protein-RNA complexes that are disrupted by small molecules will lead to a better understanding of the inhibition mechanisms possible. Indeed, as more LIRA/protein/small molecule combinations are discovered and structurally, kinetically, and thermodynamically characterized, an opportunity will exist to identify features of the protein-RNA complexes that make them susceptible to regulation by small molecules. This information will be valuable to those designing small molecule inhibitors of naturally occurring and functionally important protein-RNA complexes [40].

Significance

Several chemical genetics techniques have been developed that complement functional genetics in deciphering the cellular function of gene products [2–8, 12]. One of these approaches utilizes RNA aptamers that inhibit their target proteins in vivo [12, 15]. We have extended the utility of this approach by demonstrating that RNA inhibitors of protein function can be discovered through in vitro evolution and are released from their targets in the presence of specific small molecules (inducers). This allows for greater temporal control of the targeted protein activity, as it can be reactivated upon addition of the inducer at a specific time point. This method should prove particularly useful in defining the function of gene products involved in phenomena where the timing of events is critical, such as the cell cycle, circadian clocks, or embryonic development. In addition, in-depth studies of ligand-regulated aptamers like those described here will identify features of protein-RNA complexes that make them susceptible to regulation by small molecules.

Experimental Procedures

General

Distilled, deionized water was used for all aqueous reactions and dilutions. Biochemical reagents were obtained from Sigma/Aldrich unless otherwise noted. Restriction enzymes and nucleic acid modifying enzymes were purchased from New England Biolabs. Oligonucleotides were prepared on a Perkin Elmer/ABI Model 392 DNA/RNA synthesizer with β-cyanoethyl phosphoramidites. 5′-Dimethoxytrityl protected 2′-deoxyadenosine, 2′-deoxyguanosine, 2′-deoxycytidine, and thymidine phosphoramidites were purchased from Perkin Elmer/ABI. [γ-^{32}P]ATP (6000 Ci/mmol) and [^{32}P]pCp (3000 Ci/mmol) were obtained from DuPont NEN. Storage phosphor autoradiography was carried out using imaging plates purchased from Kodak.

A Molecular Dynamics STORM 840 was used to obtain all data from phosphorimaging plates.

Fpg Purification

E. coli Fpg was overexpressed and purified as previously described [28, 35, 36]. We estimated that the enzyme was 70% active.

Random Library Preparation

A 105 nt DNA oligonucleotide (0.2 nmol) was used as the template for a three-cycle PCR reaction, which yielded a 130 bp dsDNA product consisting of a T7 promoter and a 60-mer random region flanked by EcoRI and HindIII cloning sites. Transcription from this DNA generated a 105-nt-long random RNA pool [41].

Selections

In each round, ~2 nmol of RNA pool was denatured at 95°C in 0.5 ml of the selection buffer (1× SB: 10 mM Tris-HCl, 50 mM NaCl, 2.5 mM $MgCl_2$ [pH 7.0]) and allowed to slowly cool to room temperature. A single 13 mm filter paper disc (HAWP01300, Millipore) was added to the RNA pool, and the tube was gently mixed for 20 min. This step excluded filter paper binding RNAs. The RNA pool was then transferred to a tube with 0.3 nmol of Fpg and allowed to bind for 20 min with gentle mixing. To separate Fpg-bound from free RNA, a vacuum manifold-mounted 96-well plate with filter paper bottoms (MAVM096OR and MAHAS4510, Millipore) was used. The binding reaction was loaded into a well, and vacuum was applied for 1 min. Unbound RNAs passed through the filter, while Fpg and the bound RNAs were retained. The RNA-protein complexes were washed with 1 ml of 1× SB to remove weakly binding RNAs. In the first six rounds, the Fpg-bound RNAs were eluted with 0.2 ml of urea elution buffer (100 mM Na citrate, 7 M urea, 10 mM EDTA [pH 5.2]) which was preheated to 65°C. The eluted RNAs were washed three times with 0.5 ml water in a YM-10 microcon concentrator (Millipore), then treated with 5 units of RNase-free DNase I (Promega) for 3 hr at 37°C . Access RT-PCR kit (Promega) was used to amplify RNA winners from each round. After six rounds, the RNA pool was divided and used for two parallel selections. One selection utilized the same urea elution step as before and was performed for an additional eight rounds. The other selection employed elution buffer that consisted of 1× SB supplied with neomycin. The number of rounds in this selection (including the initial six rounds) was 23.

Cloning

The cDNA from final rounds of each selection was digested with EcoRI and HindIII (NEB), then cloned into pUC-19 vector and transformed into *E. coli* XL-1 Blue cells. Plasmids coding for individual RNA clones were isolated, sequenced, and used for production of aptamers [42].

Filter Binding Assays

Protein-RNA binding affinity was assessed using filter binding assays. These were carried out by mixing increasing concentrations of Fpg with small amounts (0.1 nM) of 5′ end-labeled aptamer, followed by incubation for 15 min at room temperature. Bound and free RNA were separated using filter paper under vacuum filtration and washing. Both the total and free (flow-through plus the wash) RNA were measured by scintillation counter, and fraction bound was calculated. The data were plotted as a function of Fpg concentration and fitted using a single-site binding equation: fraction bound = [Fpg] / ([Fpg] + K_d).

Fpg Assays

Fpg activity assays were carried out at room temperature in 1× SB under steady-state conditions with 1 nM Fpg. An 18-mer dsDNA was used as the Fpg substrate. The 8-oxo-dG-containing strand was 5′ labeled and had the following sequence: d(5′-TCATGG GTC(8-oxo-G)TCGGTATA-3′), and the complementary strand contained a cytidine opposite 8-oxo-dG. Reaction components were mixed in 18 μl and incubated for 12 min, followed by the addition of 2 μl of 200 nM DNA substrate (20 nM final). After 7 min, reactions were quenched with 15 μl of 95°C stop solution (97% formamide, 0.02% xylene cyanol in 0.2× TBE) and heated at 95°C for an additional 5 min. The reactions were resolved on 15% denaturing PAGE and visualized using phosphorimager screens. The amount of product was calculated as a percent of 20 nM substrate and without any inhibitors was measured to be approximately 2 nM under these conditions.

Secondary Structure Prediction and Testing

Secondary structure prediction was performed using the web-based MFOLD program on Dr. Michael Zuker's website, http://bioinfo.math.rpi.edu/~mfold/rna/form1.cgi [37]. Testing of the predicted structure was carried out using T1, S1, and V1 ribonuclease digests. All reactions were carried out for 10 min at room temperature in 1× SB under native conditions and in the presence of 10 μg/mL of yeast $tRNA^{Phe}$. In the case of S1 ribonuclease, reactions were supplied with 0.1 mM $ZnCl_2$ for optimal activity.

T1 Quantitative Footprinting

Footprints for both Fpg and neomycin were obtained using T1 RNase under native conditions. The reactions were performed in 1× SB at room temperature with 10 μg/mL of $tRNA^{Phe}$. Increasing amounts of Fpg or neomycin were incubated with 10 nM labeled aptamer for 10 min, followed by a 10 min enzyme digest. The reactions were quenched with 15 μl of stop solution, heat denatured, and 5 μl of each was resolved on 10% denaturing PAGE. After phosphorimaging the gel, the cleavage efficiency at G27 was calculated by subtracting the background band in the control lane and normalizing for the different loading per lane. The cleavage data were converted into binding data for neomycin, assuming that the maximum cleavage corresponds to 0% occupancy by neomycin and that the minimum cleavage corresponds to 100% occupancy by neomycin. Fraction of aptamer bound by neomycin was plotted as a function of neomycin concentration, and the data were fitted using a single-site binding equation: fraction bound = [neo] / ([neo] + K_d). The results are reported as the average and standard deviation for three different experiments.

Acknowledgments

We thank Professor Sheila David and Michael Leipold in the Department of Chemistry, University of Utah for the *E. coli* overexpression system for Fpg and for technical assistance. This work was supported by a grant from the National Institutes of Health to P.A.B. (GM-57214).

Received: June 17, 2002
Revised: July 16, 2002
Accepted: July 16, 2002

References

1. Malakoff, D. (2001). Will a smaller genome complicate the patent chase? Science *291*, 1194.
2. Specht, K.M., and Shokat, K.M. (2002). The emerging power of chemical genetics. Curr. Opin. Cell Biol. *14*, 155–159.
3. Verdugo, D.E., Cancilla, M.T., Ge, X., Gray, N.S., Chang, Y.T., Schultz, P.G., Negishi, M., Leary, J.A., and Bertozzi, C.R. (2001). Discovery of estrogen sulfotransferase inhibitors from a purine library screen. J. Med. Chem. *44*, 2683–2686.
4. Shen, K., Keng, Y.F., Wu, L., Guo, X.L., Lawrence, D.S., and Zhang, Z.Y. (2001). Acquisition of a specific and potent PTP1B inhibitor from a novel combinatorial library and screening procedure. J. Biol. Chem. *276*, 47311–47319.
5. McKenna, J.M., Halley, F., Souness, J.E., McLay, I.M., Pickett, S.D., Collis, A.J., Page, K., and Ahmed, I. (2002). An algorithm-directed two-component library synthesized via solid-phase methodology yielding potent and orally bioavailable p38 MAP kinase inhibitors. J. Med. Chem. *45*, 2173–2184.
6. Norman, T.C., Gray, N.S., Koh, J.T., and Schultz, P.G. (1996). A structure-based library approach to kinase inhibitors. J. Am. Chem. Soc. *118*, 7430–7431.
7. Kuruvilla, F.G., Shamji, A.F., Sternson, S.M., Hergenrother, P.J., and Schreiber, S.L. (2002). Dissecting glucose signaling with diversity-oriented synthesis and small-molecule microarrays. Nature *416*, 653–657.

8. Belshaw, P.J., Schoepfer, J.G., Liu, K.-Q., Morrison, K.L., Schreiber, S.L. (1995). Rational design of orthogonal receptor-ligand combinations. Angew. Chem. Int. Ed. Engl. *34*, 2129–2132.
9. Conrad, R., Keranen, L.M., Ellington, A.D., and Newton, A.C. (1994). Isozyme-specific inhibition of protein kinase C by RNA aptamers. J. Biol. Chem. *269*, 32051–32054.
10. Seiwert, S.D., Nahreini, T.S., Aigner, S., Ahn, N.G., and Uhlenbeck, O.C. (2000). RNA aptamers as pathway-specific MAP kinase inhibitors. Chem. Biol. *7*, 833–843.
11. Wilson, D.S., and Szostak, J.W. (1999). In vitro selection of functional nucleic acids. Annu. Rev. Biochem. *68*, 611–647.
12. Famulok, M., Blind, M., and Mayer, G. (2001). Intramers as promising new tools in functional proteomics. Chem. Biol. *8*, 931–939.
13. Blind, M., Kolanus, W., and Famulok, M. (1999). Cytoplasmic RNA modulators of an inside-out signal-transduction cascade. Proc. Natl. Acad. Sci. USA *96*, 3606–3610.
14. Shi, H., Hoffman, B.E., and Lis, J.T. (1999). RNA aptamers as effective protein antagonists in a multicellular organism. Proc. Natl. Acad. Sci. USA *96*, 10033–10038.
15. Thomas, M., Chedin, S., Carles, C., Riva, M., Famulok, M., and Sentenac, A. (1997). Selective targeting and inhibition of yeast RNA polymerase II by RNA aptamers. J. Biol. Chem. *272*, 27980–27986.
16. Werstuck, G., and Green, M.R. (1998). Controlling gene expression in living cells through small molecule-RNA interactions. Science *282*, 296–298.
17. McCollum, D., and Gould, K.L. (2001). Timing is everything: regulation of mitotic exit and cytokinesis by the MEN and SIN. Trends Cell Biol. *11*, 89–95.
18. Ambros, V. (2000). Control of developmental timing in Caenorhabditis elegans. Curr. Opin. Genet. Dev. *10*, 428–433.
19. Lee, R.C., and Ambros, V. (2001). An extensive class of small RNAs in Caenorhabditis elegans. Science *294*, 862–864.
20. Hermann, T., and Patel, D.J. (2000). Adaptive recognition by nucleic acid aptamers. Science *287*, 820–825.
21. Jenison, R.D., Gill, S.C., Pardi, A., and Polisky, B. (1994). High-resolution discrimination by RNA. Science *263*, 1425–1429.
22. Soukup, G.A., and Breaker, R.R. (1999). Engineering precision RNA molecular switches. Proc. Natl. Acad. Sci. USA *96*, 3584–3589.
23. Robertson, M.P., and Ellington, A.D. (2000). Design and optimization of effector-activated ribozyme ligases. Nucleic Acids Res. *28*, 1751–1759.
24. Piganeau, N., Jenne, A., Thuillier, V., and Famulok, M. (2000). An allosteric ribozyme regulated by doxycycline. Angew. Chem. Int. Ed. *39*, 4369–4373.
25. Hartig, J.S., Najafi-Shoushtari, S.H., Grune, I., Yan, A., Ellington, A.D., and Famulok, M. (2002). Protein-dependent ribozymes report molecular interactions in real time. Nat. Biotechnol. *20*, 717–722.
26. Koizumi, M., Soukup, G.A., Kerr, J.N.Q., and Breaker, R.R. (1999). Allosteric selection of ribozymes that respond to the second messengers cGMP and cAMP. Nat. Struct. Biol. *6*, 1062–1071.
27. Chetsanga, C.J., and Lindahl, T. (1979). Release of 7-methylguanine residues whose imidazole rings have been opened from damaged DNA by a DNA glycosylase from Escherichia coli. Nucleic Acids Res. *10*, 3673–3684.
28. Boiteux, S., O'Connor, T.R., Lederer, F., Gouyette, A., and Laval, J. (1990). Homogeneous Escherichia coli FPG protein. A DNA glycosylase which excises imidazole ring-opened purines and nicks DNA at apurinic/apyrimidinic sites. J. Biol. Chem. *265*, 3916–3922.
29. David, S.S., and Williams, S.D. (1998). Chemistry of glycosylases and endonucleases involved in base-excision repair. Chem. Rev. *98*, 1221–1261.
30. Tchou, J., Kasai, H., Shibutani, S., Chung, M.H., Laval, J., Grollman, A.P., and Nishimura, S. (1991). 8-oxoguanine (8-hydroxyguanine) DNA glycosylase and its substrate specificity. Proc. Natl. Acad. Sci. USA *88*, 4690–4694.
31. Moazed, D., and Noller, H.F. (1987). Interaction of antibiotics with functional sites in 16S ribosomal RNA. Nature *327*, 389–394.
32. Yoshizawa, S., Fourmy, D., Eason, R.G., and Puglisi, J.D. (2002). Sequence-specific recognition of the major groove of RNA by deoxystreptamine. Biochemistry *41*, 6263–6270.
33. Carter, A.P., Clemons, W.M., Brodersen, D.E., Morgan-Warren, R.J., Wimberly, B.T., and Ramakrishnan, V. (2000). Functional insights from the structure of the 30S ribosomal subunit and its interactions with antibiotics. Nature *407*, 340–348.
34. Wallis, M.G., von Ahsen, U., Schroeder, R., and Famulok, M. (1995). A novel RNA motif for neomycin recognition. Chem. Biol. *2*, 543–552.
35. Leipold, M.D., Muller, J.G., Burrows, C.J., and David, S.S. (2000). Removal of hydantoin products of 8-oxoguanine oxidation by the Escherichia coli DNA repair enzyme, FPG. Biochemistry *39*, 14984–14992.
36. Zharkov, D.O., Rieger, R.A., Iden, C.R., and Grollman, A.P. (1997). NH2-terminal proline acts as a nucleophile in the glycosylase/ AP-lyase reaction catalyzed by Escherichia coli formamidopyrimidine-DNA glycosylase (Fpg) protein. J. Biol. Chem. *272*, 5335–5342.
37. Mathews, D.H., Sabina, J., Zuker, M., and Turner, D.H. (1999). Expanded sequence dependence of thermodynamic parameters improves prediction of RNA secondary structure. J. Mol. Biol. *288*, 911–940.
38. Leach, B.E., DeVries, W.H., Nelson, H.A., Jackson, W.G., and Evans, J.S. (1951). The isolation and characterization of neomycin. J. Am. Chem. Soc. *73*, 2797–2800.
39. Ellington, A.D., and Szostak, J.W. (1990). In vitro selection of RNA molecules that bind specific ligands. Nature *346*, 818–822.
40. Hermann, T. (2000). Strategies for the design of drugs targeting RNA and RNA-protein complexes. Angew. Chem. Int. Ed. *39*, 1890–1905.
41. Abelson, J.N. (1996). Combinatorial chemistry. Methods Enzymol. *267*, 291–335.
42. Sambrook, J., Fritsch, E.F., and Maniatis, T. (1989). Molecular Cloning: A Laboratory Manual (Cold Spring Harbor, NY: Cold Spring Harbor Laboratory Press).